

# Hypernuclear production by $(\gamma, K^+)$ reaction within a relativistic model

R. Shyam<sup>1,2</sup>, H. Lenske<sup>2</sup>, and U. Mosel<sup>2</sup>

<sup>1</sup>*Saha Institute of Nuclear Physics, Kolkata, India*

<sup>2</sup>*Institute für Theoretische Physik, Universität Giessen, D-35292 Giessen, Germany*

(Dated: November 20, 2018)

## Abstract

Within a fully covariant model based on an effective Lagrangian picture, we investigate the hypernuclear production in photon-nucleus interaction on  $^{16}\text{O}$  target. The explicit kaon production vertex is described via creation, propagation and decay into relevant channel of  $N^*(1650)$ ,  $N^*(1710)$ , and  $N^*(1720)$  intermediate baryonic resonance states in the initial interaction of the incident photon with one of the target protons. Bound state nucleon and hyperon wave functions are obtained by solving the Dirac equation. Using vertex parameters determined in the previous studies, contributions of the  $N^*(1710)$  baryonic resonance dominate the total production cross sections which are found to peak at photon energies below 1 GeV. The results show that photo-production is the most appropriate means for studying the unnatural parity hypernuclear states, thus accessing the spin dependence of the hyperon-nucleon interaction.

PACS numbers: 21.80.+a, 13.60.-r, 13.75.Jz

Lambda hypernuclei are the most extensively studied hypernuclear systems, both experimentally (see, e.g., a recent review [1]) as well as theoretically [2, 3, 4]. They have, traditionally, been produced by stopped as well as in-flight ( $K^-$ ,  $\pi^-$ ) and ( $\pi^+$ ,  $K^+$ ) reactions. Alternatively,  $\Lambda$ -hypernuclei can also be produced with proton as well as electromagnetic probes. The feasibility of hypernuclear production with proton beams has been investigated in Refs. [5, 6]. Recently, discrete hypernuclear states have been produced for the first time in electron induced reactions on light nuclear targets at the Jlab [7, 8, 9]. First measurements of the ( $\gamma$ ,  $K^+$ ) reaction on a nuclear target ( $^{12}\text{C}$ ) have been reported long ago [10, 11]. Interest in this field has been revived as a number of experiments are planned for this reaction at accelerators MAMI-C in Mainz, ELSA in BONN and also at Jlab (see, e.g., Ref. [12]). In this paper we report a theoretical study of the ( $\gamma$ ,  $K^+$ ) reaction on a  $^{16}\text{O}$  target.

In contrast to the hadronic reactions [( $K^-$ ,  $\pi^-$ ), and ( $\pi^+$ ,  $K^+$ )] which are confined mostly to the nuclear surface due to strong absorption of both  $K^-$  and  $\pi^\pm$ , the ( $\gamma$ ,  $K^+$ ) reaction occurs deep in the nuclear interior due to weaker interactions of both photon and  $K^+$  with the nucleus. This property makes this reaction an ideal tool for studying the deeply bound hypernuclear states provided the corresponding production mechanism is reasonably well understood. Unlike the hadronic reactions which excite predominantly the natural parity hypernuclear states, both unnatural and natural parity states are excited with comparable strength in the ( $\gamma$ ,  $K^+$ ) reaction. This is because sizable spin-flip amplitudes are present in the elementary  $p(\gamma, K^+)\Lambda$  reaction due to the fact that the photon has spin 1 and small angles dominate this reaction. This feature persists in the hypernuclear photoproduction. Furthermore, Since, a proton in the target nucleus is converted into a hyperon, this reaction leads to the production of neutron rich hypernuclei (see, e.g., Ref. [13]) which may carry exotic features such as a halo structure.

Several theoretical investigations of the ( $\gamma$ ,  $K^+$ ) reaction on nuclear targets have been reported in the literature [14, 15, 16, 17, 18, 19, 20]. In these studies, the kaon photoproduction amplitudes on nuclei are calculated within an impulse approximation by determining expectation values of the operator for the elementary  $p(\gamma, K^+)\Lambda$  production process between initial and final states of the reaction. This operator is constructed either by using the Feynman diagrammatic approach where graphs corresponding to Born terms and resonance terms in  $s$  and  $u$  channels, are included [15, 16, 20, 21], or phenomenologically by parameterizing the experimental cross sections for the elementary process [18, 19]. Although in Ref. [17],

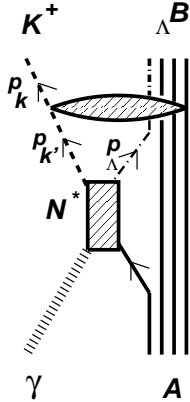


FIG. 1: Representation of the type of Feynman diagrams included in our calculations. The elliptic shaded area represents the optical model interactions in the outgoing channel.

Dirac spinors have been used for bound state wave functions in the initial and final channels, a full covariant calculation of this reaction is still missing.

In this paper, we study the  $A(\gamma, K^+)_{\Lambda}B$  reaction within a fully covariant model by retaining the field theoretical structure of the interaction vertices and by treating the baryons as Dirac particles moving in a static nuclear mean-field. This type of approach has previously been used in Ref. [6] to describe the hypernuclear production in proton-nucleus collisions. In our model, the initial state interaction of the incoming photon with a bound proton leads to excitations of  $N^*(1650) [\frac{1}{2}^-]$ ,  $N^*(1710) [\frac{1}{2}^+]$ , and  $N^*(1720) [\frac{3}{2}^+]$  baryonic resonance intermediate states which are shown to make predominant contributions to  $p(\gamma, K^+)_{\Lambda}$  cross sections in similar effective Lagrangian studies [22, 23]. Terms involving nucleon intermediate states (Born terms) have not been considered here as their contributions are found [20] to be insignificant to both elementary as well as in medium (on  $^{12}\text{C}$  nucleus) photo-kaon production reactions.

We have considered the diagrams of the type shown in Fig. 1 which implies that our model has only the  $s$ -channel resonance contributions. In principle,  $u$ -channel and  $t$ -channel contributions should also be included. However, calculations of the  $u$ -channel contributions would require the knowledge of *a priori* unknown couplings to the strange baryonic resonances. That is why these graphs have been ignored in recent photo-kaon production studies [22, 23]. The  $t$ -channel diagrams contribute to the non-resonant background and may be required if the nucleon intermediate states are considered. In fact, it has been shown that [20] for the elementary photoproduction reaction, Born plus vector meson  $t$ -channel

contributions become relatively large at photon energies in excess of 2.1 GeV [20]. Since, in this paper we have concentrated only on investigating the role of baryonic resonances in the  $(\gamma, K^+)$  reaction and have ignored the nucleon intermediate states, we have omitted these terms to keep our model as simple as possible. Furthermore, in this exploratory study, to reduce the further computational complications we have used plane waves (PW) to describe the relative motion of the outgoing kaon which is justified by the relatively weaker mutual interaction in this channel.

The effective Lagrangians for the electromagnetic couplings of spin- $\frac{1}{2}$  resonances are given by [24]

$$\mathcal{L}_{N_{1/2}^* N \gamma} = \left( \frac{eg_{N^* N \gamma}^1}{4m_N} \right) \bar{\Psi}_{N^*} \Gamma_{\mu\nu} \Psi_N F^{\mu\nu} + h.c., \quad (1)$$

where the operator  $\Gamma_{\mu\nu}$  is  $\gamma_5 \sigma_{\mu\nu}$  ( $\sigma_{\mu\nu}$ ) for odd (even) parity resonances.  $F_{\mu\nu}$  represents the electromagnetic field tensor:  $F_{\mu\nu} = \partial_\nu A_\mu - \partial_\mu A_\nu$ . We have used the notations of Ref. [25] through out in this paper. For the spin- $\frac{3}{2}$  case, we have

$$\begin{aligned} \mathcal{L}_{N_{3/2}^* N \gamma} &= \left( \frac{eg_{N^* N \gamma}^1}{2m_N} \right) \bar{\Psi}_{N^*}^\alpha \Theta_{\alpha\mu}(z1) \gamma_\nu \Gamma \Psi_N F^{\mu\nu} \\ &\quad - \left( \frac{eg_{N^* N \gamma}^2}{4m_N^2} \right) \bar{\Psi}_{N^*}^\alpha \Theta_{\alpha\mu}(z2) \Gamma (\partial_\nu \Psi_N) F^{\mu\nu} \\ &\quad + h.c., \end{aligned} \quad (2)$$

In Eq. (2), the operator  $\Gamma$  is unity and  $\gamma_5$  for odd and even parity resonances, respectively.  $\Psi_\mu^{N^*}$  is the vector spinor for the spin- $\frac{3}{2}$  particle. This involves the off shell projector  $\Theta_{\alpha\mu}(z) = g_{\alpha\mu} - \frac{1}{2}(1+2z)\gamma_\alpha\gamma_\mu$  where  $z$  is the off-shell parameter [24] which describes the off-shell admixture of spin- $\frac{1}{2}$  fields. The choice of this parameter is arbitrary and in earlier studies it has been treated as a free parameter to be determined by fitting to the data (see, e.g. [22]). For a more detailed discussion we refer to [22, 26, 27]. The electromagnetic coupling constants  $g_1, g_2$  are related to the helicity couplings  $[A_{1/2,3/2}]$  (see, e.g. Ref [24]) which are taken from Ref. [22]. There these are determined in a coupled channels K-matrix method by fitting simultaneously to all the available data for transitions from  $\gamma N$  to five meson-baryon final states,  $\pi N$ ,  $\pi\pi N$ ,  $\eta N$ ,  $K\Lambda$ , and  $K\Sigma$  for center of mass energies ranging from threshold to 2 GeV including all the baryonic resonances up to spin  $\leq \frac{3}{2}$  and excitation energies 2 GeV.

For the resonance-hyperon-kaon vertices we have

$$\mathcal{L}_{N_{1/2}^* \Lambda K^+} = -g_{N_{1/2}^* \Lambda K^+} \bar{\Psi}_{N^*} i \Gamma' \boldsymbol{\tau} \boldsymbol{\Phi}_{K^+} \Psi + h.c.. \quad (3)$$

TABLE I: Coupling constants for the  $N^*\Lambda K$  vertices and the helicity amplitudes used in the calculations [22, 28].

vertex	$g$	$A_{1/2}$ ( $10^{-3}GeV^{-1/2}$ )	$A_{3/2}$ ( $10^{-3}GeV^{-1/2}$ )
$N^*(1710)N\gamma$	—	44	—
$N^*(1710)\Lambda K^+$	6.12	—	—
$N^*(1650)N\gamma$	—	49	—
$N^*(1650)\Lambda K^+$	0.76	—	—
$N^*(1720)N\gamma$	—	18	-19
$N^*(1720)\Lambda K^+$	0.87	—	—

$$\mathcal{L}_{N_{3/2}^*\Lambda K^+} = \frac{g_{N_{3/2}^*\Lambda K^+}}{m_{K^+}} \bar{\Psi}^{\mu N^*} \Gamma \boldsymbol{\tau} \cdot \partial^\mu \boldsymbol{\Phi}_{K^+} \Psi + \text{h.c.} \quad (4)$$

In Eq. (4), the operator  $\Gamma$  is  $\gamma_5$  (unity) for even (odd) parity resonance. Signs and values of the hyperon-resonance-kaon coupling constants ( $g_{N^*YK}$ ) have been taken from [28] which along with the helicity amplitudes are shown in Table I. Values of  $g_{N^*YK}$  used by us are also consistent with those reported in Ref. [22]. It may be noted that we have used a pseudoscalar (PS) coupling for the resonance-hyperon-kaon vertex. Differences between pseudovector and PS couplings are expected to be small [22, 29]. The propagators for spin- $\frac{1}{2}$  and spin- $\frac{3}{2}$  resonances are taken to be the same as those described in Ref. [6].

After having established these ingredients, one can write down, by following the well known Feynman rules, the amplitudes for graphs of the type shown in Fig. 1. We have employed pure single-particle-single-hole ( $(\Lambda N^{-1})$ ) wave functions to describe the nuclear structure part because configuration mixing terms are expected to be small. The nuclear structure part is treated exactly in the same way as is described in Ref. [17]. Amplitudes involve momentum space four component (spin space) Dirac spinors ( $\psi$ ) which represent wave functions of nucleon and hyperon bound states [30] and the momentum space kaon-nucleus wave function  $[\phi_K^{(-)*}(p'_K, p_K)]$  which can be calculated by using an appropriate  $K^+$ -nucleus optical potential (see, *e.g.*, Ref. [31]). Momentum  $p_K$  represents the asymptotic free state while  $p'_K$  is the momentum coordinate of the produced kaon as shown in Fig. 1. In the PW approximation, one writes  $\Phi_K^{(-)*}(p'_K, p_K) = \delta^4(p'_K - p_K)$ . We include energy dependent

widths in denominators of resonance propagators to account for the fact that they have finite lifetime for decay into various channels.

Spinors  $\psi(p)$  are solutions of the Dirac equation in momentum space for a bound state problem in the presence of an external potential field [6, 30]

$$\not{p}\psi(p) = m_N\psi(p) + F(p), \quad (5)$$

where

$$F(p) = \delta(p_0 - E) \left[ \int d^3p' V_s(-\mathbf{p}') \psi(\mathbf{p} + \mathbf{p}') - \gamma_0 \int d^3p' V_v^0(-\mathbf{p}') \psi(\mathbf{p} + \mathbf{p}') \right]. \quad (6)$$

In Eq. (6), the real scalar and timelike vector potentials  $V_s$  and  $V_v^0$  represent, respectively, the momentum space local Lorentz covariant interaction of single nucleon or  $\Lambda$  with the remaining  $(A - 1)$  nucleons. We denote a four momentum by  $p = (p_0, \mathbf{p})$ . The magnitude of the three momentum  $\mathbf{p}$  is represented by  $k$ , and its directions by  $\hat{p}$ .  $p_0$  is the time like component of  $p$ . Spinors  $\psi(p)$  and  $F(p)$  are written as

$$\begin{aligned} \psi(p) &= \delta(p_0 - E) \begin{pmatrix} f(k) \mathcal{Y}_{\ell 1/2 j}^{m_j}(\hat{p}) \\ -i g(k) \mathcal{Y}_{\ell' 1/2 j}^{m_j}(\hat{p}) \end{pmatrix}, \\ F(p) &= \delta(p_0 - E) \begin{pmatrix} \zeta(k) \mathcal{Y}_{\ell 1/2 j}^{m_j}(\hat{p}) \\ -i \zeta'(k) \mathcal{Y}_{\ell' 1/2 j}^{m_j}(\hat{p}) \end{pmatrix}, \end{aligned} \quad (7)$$

where  $f(k)[\zeta(k)]$  is the radial part of the upper component of the spinor  $\psi(p)[F(p)]$ . Similarly  $g(k)[\zeta'(k)]$  are the same of their lower component.  $f(k)$  and  $g(k)$  represent Fourier transforms of radial parts of the corresponding coordinate space spinors.  $\zeta(k)$  are related to  $f$ ,  $g$  and the scalar and vector potentials (see Ref. [30] for more details). We have defined  $\ell' = 2j - \ell$  with  $\ell$  and  $j$  being the orbital and total angular momenta, and

$$\mathcal{Y}_{\ell 1/2 j}^{m_j}(\hat{p}) = \sum_{m_\ell \mu} \langle \ell m_\ell 1/2 \mu | j m_j \rangle Y_{\ell m_\ell}(\hat{p}) \chi_{1/2 \mu},$$

where  $Y$  represents the spherical harmonics and  $\chi_{1/2 \mu}$  the spin space wave function of a spin- $\frac{1}{2}$  particle.

Since our analysis is carried out all along in the momentum space, it includes all the nonlocalities in the production amplitude that arise from the resonance propagators. The differential cross section for the  $(\gamma, K^+)$  reaction is given by

$$\frac{d\sigma}{d\Omega} = \frac{1}{4(2\pi)^2} \frac{m_A m_B}{(E_\gamma + E_A)^2} \frac{p_K}{p_\gamma} \sum_{M_i M_f \epsilon} \left| \sum_R T_{M_i M_f, \epsilon} \right|^2,$$

where  $E_\gamma$  and  $E_A$  are the total energies of incident photon and the target nucleus, respectively while  $m_A$  and  $m_B$  are the masses of the target and residual nuclei, respectively.  $\sum_R$  represents summation over all the resonances.  $M_i$  and  $M_f$  are initial and final spin states, respectively, and  $\epsilon$  is the photon polarization.

We have chosen the reaction  $^{16}\text{O}(\gamma, K^+)^{16}_\Lambda\text{N}$  for the first numerical application of our model, as this reaction is well known to have a simple structure. The initial state is a doubly closed system. The binding energies (BE) of  $1s_{1/2}$ ,  $1p_{3/2}$  and  $1p_{1/2}$  single particle states in  $^{16}_\Lambda\text{N}$  hypernucleus are taken to be 13.20 MeV, 2.50 MeV and 2.04 MeV, respectively which are the same as those given in Ref. [17]. The BE of the  $1p_{3/2}$  and  $1p_{1/2}$  nucleon hole states in  $^{16}\text{O}$  are taken as 18.40 MeV and 12.13 MeV, respectively [18]. Because of the large separation in the binding energies of the nucleon hole states, the hypernuclear spectrum is clearly divided into 4 groups corresponding to configurations  $[p_{1/2}^{-1}, s_\Lambda]$ ,  $[p_{3/2}^{-1}, s_\Lambda]$ ,  $[p_{1/2}^{-1}, p_\Lambda]$ , and  $[p_{3/2}^{-1}, p_\Lambda]$ . The configuration mixing is negligible except may be for the  $J^\pi = 1^+$  hypernuclear state. Any  $\Lambda N$  residual interaction that may lead to configuration mixing as considered in Ref. [32] is neglected in our study.

Spinors  $\psi(p)$  for bound hypernuclear and nucleon states are obtained by Fourier transformations of the corresponding coordinate space spinors which are determined by solving the Dirac equation with scalar and vector potential fields ( $V_s$  and  $V_v$ , respectively) with a Woods-Saxon radial form with (reduced radius)  $r_s = r_v = 0.983$  fm, and (diffuseness)  $a_s = 0.70$  fm and  $a_v = 0.58$  fm. For a given state, the depths of these fields ( $V_s^0$  and  $V_v^0$ ) have been searched so as to reproduce the BE of that state. For the single particle  $\Lambda$  states  $1s_{1/2}$ ,  $1p_{3/2}$  and  $1p_{1/2}$  the values of ( $V_s^0$  and  $V_v^0$ ) were (-204.78 MeV and 165.89 MeV), (-228.49 MeV and 185.96 MeV), and (-251.80 and 203.96 MeV), respectively, while for each of the nucleon hole states  $1p_{3/2}$  and  $1p_{1/2}$ , they were (-445.0 MeV and 360 MeV). We see that the strengths of the mean field self energies for the  $\Lambda$  states are about 1/2 of those of the nucleon states which is line with the results of the microscopic Dirac-Bruckner calculations as shown in Ref. [4].

It is shown in Ref. [30] that spinors calculated in this way provide a good description of the experimental nucleon momentum distributions for various nucleon orbits. Fig. 2 shows, e.g., the momentum space  $1p_{1/2}$   $\Lambda$  and  $1p_{3/2}$   $\Lambda$  hyperon spinors as functions of the momentum transfer ( $q$ ), for the  $^{16}_\Lambda\text{N}$  hypernucleus. In the lower panel of Fig. 2 we show the momentum distribution of the  $\Lambda$  hyperon for these states in  $^{16}_\Lambda\text{N}$ . We note that only for  $q < 1.5 fm^{-1}$ , is

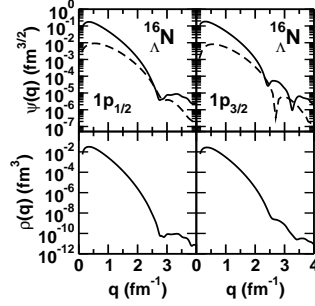


FIG. 2: (Upper panel) Magnitudes of the upper ( $|f(q)|$ ) (full line) and lower ( $|g(q)|$ ) (dashed line) components of the momentum space spinors for  $1p_{3/2} \Lambda$  and  $1p_{1/2} \Lambda$  orbits in  $^{16}\Lambda\text{N}$  hypernucleus. (Lower panel) hyperon momentum distributions (defined as  $\rho(q) = [|f(q)|^2 + |g(q)|^2]$ ) for the same states.

the magnitude of the lower component ( $|g(q)|$ ) substantially smaller than that of the upper component ( $|f(q)|$ ). In the region of  $q$  pertinent to the kaon production,  $|g(q)|$  may not be negligible. In fact, it has been shown earlier [17] that the relativistic effects resulting from the small component of Dirac bound states are large for the kaon photoproduction reactions on nuclei.

The threshold for the kaon photoproduction on  $^{16}\text{O}$  is about 680 MeV. The momentum transfer involved in this reaction at zero degrees is above 500 MeV/c. In Fig. 3, we investigate the contributions of the various resonance intermediate states to the total cross section for populating the  $(1p_{3/2}^{-1}, 1s_{1/2}^{\Lambda})2^{-}$  state in the  $^{16}\text{O}(\gamma, K^{+})^{16}\Lambda\text{N}$  reaction as a function of photon energy. We see that the individual contributions of the  $N^{*}(1710)$  intermediate state by far dominate the cross sections. In comparison to this, cross sections corresponding to the  $N^{*}(1650)$  state are at least one order magnitude smaller and those of the  $N^{*}(1720)$  state are smaller by 3-4 orders of magnitude (these contributions are omitted from this figure consequently). The nearly negligible contribution of this resonance has also been noted in the study of  $A(p, K^{+})_{\Lambda}B$  reaction [6]. It is worthwhile to note that in Ref. [20] individual contributions of various resonances are not specified although the resonance terms as a whole are shown to dominate both elementary and nuclear photo-kaon production cross sections.

Another noteworthy aspect of Fig. 3 is that cross sections peak at photon energies around 900 MeV, which is about 200 MeV above the production threshold for this reaction. Interestingly, the total cross section of the elementary  $p(\gamma, K^{+})\Lambda$  reaction also peaks about



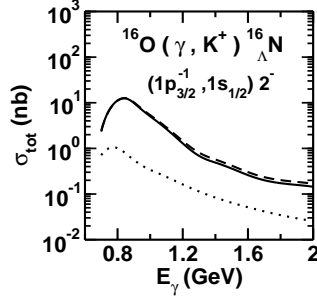


FIG. 3: Individual contributions of  $N^*(1710)$  (dashed line) and  $N^*(1650)$  (dotted line) resonance states to the total cross section for the  $^{16}\text{O}(p, K^+)\Lambda^N$  reaction for the indicated configuration as a function of photon energy. The solid line shows the coherent sum of the contributions of these two and  $N^*(1720)$  resonance states. The individual contributions of the  $N^*(1720)$  resonance are 3-4 four orders of magnitude smaller and are not shown here separately.

the same energy above the corresponding production threshold ( 910 MeV). Although the absolute magnitude of our near peak energy cross sections are comparable to those reported in Ref. [17], their drop off with the beam energy is faster than those of these authors. Such a strong drop of the cross sections with beam energy beyond the peak position was also seen in the calculations of  $(p, K^+)$  reactions on nuclei within a similar model. It may partly be due to lack of the kaon-nucleus distortion effects in our calculations. It should be mentioned here that calculations performed with only the upper component of the bound state is about 6-8% smaller than the total cross sections shown in Fig. 3. Larger effects of the lower components are seen in the angular distributions at larger angles. However, since cross sections are quite small at these angles in comparison to those at smaller ones, the total cross sections shows less sensitivity to the lower component. More comprehensive investigation of the relativistic effects due to the lower component is made in Refs. [17] where it is shown that the cross sections obtained by using fully relativistic small component are significantly different from those where the small component is related to the large component by a free space relation. It is also found that the differences between cross sections obtained by using Dirac or Schrödinger solutions for the upper component are non-negligible.

In Fig 4, we present the excitation spectrum for four groups of  $(\Lambda N^{-1})$  hypernuclear states involving bound  $1s$  and  $1p$   $\Lambda$  orbitals in the hypernucleus  $^{16}_\Lambda\text{N}$ . The relative excitation strengths for a given  $J$  state of each group of  $[(nlj)_p^{-1}, (nlj)^\Lambda]$  configuration, are obtained

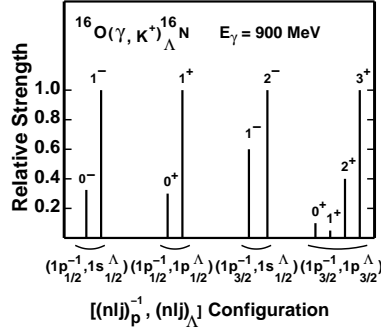


FIG. 4: Bound state excitation spectrum of hypernucleus  $^{16}\Lambda\text{N}$ .

by dividing the total cross section of that  $J$  state by that of the state having the maximum cross section within that group. We first note that within each group the highest  $J$  state is most strongly excited which is in line with the results presented in Refs. [17, 32]. Furthermore, unnatural parity states within each group [except for the ground state  $(1p_{1/2}^{-1}, 1s_{1/2}^{\Lambda})$  configuration], are preferentially excited by this reaction. For example, within the group  $(1p_{3/2}^{-1}, 1p_{3/2}^{\Lambda})$ , cross section of the  $3^+$  state is larger than that of the  $2^+$  state by about a factor of 2.5 and by more than an order of magnitude than that of the  $0^+$  state. The unnatural parity states are excited through the spin flip process. Thus, kaon photoproduction on nuclei is an ideal tool to investigate the structure of unnatural parity hypernuclear states. The addition of unnatural parity states to the spectrum of hypernuclei is expected to constrain the spin dependent part of the effective  $\Lambda - N$  interaction more tightly.

In summary, we studied the hypernuclear production by  $(\gamma, K^+)$  reaction on  $^{16}\text{O}$  within a covariant model where in the initial collision of the photon with a target proton,  $N^*(1710)$ ,  $N^*(1650)$  and  $N^*(1720)$  baryonic resonances are excited which subsequently propagate and decay into a  $\Lambda$  hyperon which gets captured in one of the nuclear orbits, and a  $K^+$  which goes out. Wave functions of nucleon and  $\Lambda$  bound states are obtained by solving the Dirac equation with appropriate potential fields. The distortion effects in the  $K^+$  channel have not been included in this study. However, as shown in Refs. [17, 32], these effects are weak for reactions on  $p$ -shell nuclei but they may be more significant for heavier systems. Since, we have not included the nucleon intermediate states (Born terms), the absolute magnitudes of our total cross sections may be uncertain to the extent of about 10%.

Using the vertex constants determined in previous studies, the excitation of  $N^*(1710)$  resonance dominates the hypernuclear production process. Similar results were also found

in the previous studies of the  $A(p, K^+)_{\Lambda}B$  reaction. The total production cross sections peak at photon energies which are above the corresponding production threshold by almost the same amount of energy as is the position of the maximum in the elementary cross section away from its respective threshold.

Our calculations confirm that the  $(\gamma, K^+)$  reaction on nuclei selectively excites the high spin unnatural parity states, which makes it an ideal tool for investigating the spin-flip transitions which are only weakly excited in reactions induced by hadronic probes. Therefore, electromagnetic hypernuclear production provides a fuller knowledge of hypernuclear spectra and will impose more severe constraints on the models of the  $\Lambda N$  interaction, particularly on its the poorly known spin dependent part. To this end it is important to extend our model to include distortion effects in the final channel so that the mechanism of this reaction can be understood more properly.

This work has been supported by Sonderforschungsbereich/Transregio 16, Bonn-Giessen-Bochum of the German Research Foundation. One of the authors (RS) acknowledges the support of Abdus Salam International Centre for Theoretical Physics in form of a senior associateship award.

- 
- [1] O. Hashimoto and H. Tamura, *Progr. Part. Nucl. Phys.* **57**, 564 (2006).
  - [2] H. Bando, T. Motoba, J. Zofka, *Int. J. Mod. Phys.* **5**, 2021 (1990).
  - [3] H. Nemura, Y. Akaishi, and Y. Suzuki, *Phys. Rev. Lett.* **89**, 142504 (2002). D. Vretenar, W. Poschl, G. A. Lalazissis, and P. Ring, *Phys. Rev. C* **57**, R1060 (1998).
  - [4] C. M. Keil, F. Hoffmann, and H. Lenske, *Phys. Rev. C* **61**, 064309 (2000); C. M. Keil and H. Lenske, *Phys. Rev. C* **66**, 054307 (2002).
  - [5] J. Kingler et al., *Nucl. Phys.* **A634**, 325 (1998).
  - [6] R. Shyam, H. Lenske and U. Mosel, *Phys. Rev. C* **69**, 065205 (2004); *ibid*, *Nucl. Phys.* **A764**, 313 (2006).
  - [7] T. Miyoshi et al., *Phys. Rev. Lett.* **90**, 232502 (2003).
  - [8] L. Yuan et. al., *Phys. Rev. C* **73**, 044607 (2006).
  - [9] M. Iodice et al., *Phys. Rev. Lett.* **99**, 052501 (2007).
  - [10] K. Maeda et al., *Nucl. Phys.* **A577**, 277c (1994).

- [11] H. Yamazaki et al., Phys. Rev. C **52**, R1157 (1995).
- [12] J. Pochodzalla, Nucl. Phys. A754, 430c (2005).
- [13] T. Bressani et al., Nucl. Phys. **A754**, 410c (2005).
- [14] A.M. Bernstein, T.W. Donnelly, and G.N. Epstein, Nucl. Phys. **A358**, 195c(1981).
- [15] S.S. Hsiao and S. R. Cotanch, Phys. Rev. C **28**, 1668 (1983).
- [16] J. Cohen, Phys. Rev. C **37**, 187 (1988).
- [17] C. Bennhold and L.E. Wright, Phys. Rev. C **39**, 927 (1989); *ibid*, Phys. Lett. **B191**, 11 (1987).
- [18] T. Motoba, M. Sotona, and K. Itonaga, Progr. Theo. Phys. (suppl) **117**, 123 (1994).
- [19] T.-S. H. Lee, Z.-Y. Ma, B. Saghai, and H. Toki, Phys. Rev. C **58**, 1551 (1998).
- [20] F.X. Lee, T. Mart, C. Bennhold, H. Habermehl, and L. E. Wright, Nucl. Phys. **A695**, 237 (2001).
- [21] R.A. Adelseck, C. Bennhold, and L.E. Wright, Phys. Rev. C **32**, 1681 (1985).
- [22] G. Penner and U. Mosel, Phys. Rev. C **66**, 055211 (2002); **66**, 055212 (2002).
- [23] V. Shklyar, H. Lenske and U. Mosel, Phys. Rev. C **72**, 015210 (2005).
- [24] T. Feuster and U. Mosel, Phys. Rev. C **58**, 457 (1998); *ibid*, Phys. Rev. C **59**, 460 (1999).
- [25] J. D. Bjorken and S. D. Drell, *Relativistic Quantum Mechanics*, (McGraw-Hill, New York, 1964).
- [26] R. Shyam, Phys. Rev. C **60**, 055213 (1999).
- [27] V. Pascalusta and O. Scholten, Nucl. Phys. A **591**, 658 (1995).
- [28] R. Shyam, Phys. Rev. C **73**, 035211 (2006).
- [29] C. Bennhold and L.E. Wright, Phys. Rev. C **36**, 438 (1987).
- [30] R. Shyam, W. Cassing and U. Mosel, Nucl. Phys. A**586**, 557 (1995); R. Shyam, A. Engel, W. Cassing, and U. Mosel, Phys. Lett. **B273**, 26 (1991).
- [31] A. S. Rosenthal and F. Tabakin, Phys. Rev. C **22** (1980) 711;
- [32] A. S. Rosenthal et al., Ann. Phys. (N.Y.) **184**, 33 (1988).